Estimates of Kinetic Energy Dissipation under Breaking Waves*

E. A. TERRAY,[†] M. A. DONELAN,[#] Y. C. AGRAWAL,[@] W. M. DRENNAN,[#] K. K. KAHMA,[‡] A. J. WILLIAMS III,[†] P. A. HWANG,[**] AND S. A. KITAIGORODSKII[‡]

[†]*Department of Applied Ocean Physics and Engineering, Woods Hole Oceanographic Institution, Woods Hole, Massachusetts*
[#]*National Water Research Institute, Canada Centre for Inland Waters, Burlington, Ontario, Canada*
[@]*Sequoia Scientific Inc., Mercer Island, Washington*
[‡]*Finnish Institute of Marine Research, Helsinki, Finland*
[**]*Naval Research Laboratory, Stennis Space Center, Mississippi*

(Manuscript received 18 April 1994, in final form 13 October 1995)

ABSTRACT

The dissipation of kinetic energy at the surface of natural water bodies has important consequences for many physical and biochemical processes including wave dynamics, gas transfer, mixing of nutrients and pollutants, and photosynthetic efficiency of plankton. Measurements of dissipation close to the surface obtained in a large lake under conditions of strong wind forcing are presented that show a layer of enhanced dissipation exceeding wall layer values by one or two orders of magnitude. The authors propose a scaling for the rate of dissipation based on wind and wave parameters, and conclude that the dissipation rate under breaking waves depends on depth, to varying degrees, in three stages. Very near the surface, within one significant height, the dissipation rate is high (an order of magnitude greater than that predicted by wall layer theory) and roughly constant. Below this is an intermediate region where the dissipation decays as z^{-2}. The thickness of this layer (relative to the significant wave height) is proportional to the energy flux from breaking normalized by ρu_*^3, which for young waves is proportional to wave age. At sufficient depth the dissipation rate asymptotes to values commensurate with a traditional wall layer. The total energy flux into the water column can be an order of magnitude greater than the conventional estimate of $\rho u_*^3/2$ and depends strongly on wave age. These results imply a pronounced shift in our approach to estimating kinetic energy dissipation in wave-stirred regions and in the modeling of various physical, chemical, and biological processes.

1. Introduction

The rate of turbulent kinetic energy dissipation, ϵ, in the upper oceanic layers and, in particular, its distribution near the surface are of great significance in matters relating to the mixing of near surface waters, mass transfer across the interface, dispersal of buoyant pollutants, testing of similarity hypotheses related to turbulent structure, and the modeling of thermocline development, among others. It is therefore not surprising that in recent years a great deal of effort has been directed toward determining its near-surface vertical distribution. Estimates of dissipation near the top of the water column have been made from three distinctly different types of platforms, that is (i) fixed towers, (ii) horizontally or nearly horizontally moving vehicles (ships, submarines, and towed bodies), and (iii) vertically profiling devices driven by a buoyancy difference. Only in rare cases has the dissipation been estimated from the smallest scales where the conversion of mechanical energy to heat occurs. More often the spectral density at intermediate scales is employed, via the Kolmogorov similarity hypothesis, to estimate the rate at which energy flows from the (large scale) source to the (small scale) sink. Occasionally, dissipation is inferred indirectly on the basis of some assumption about the energy budget—for example, that shear production and dissipation are in balance. Most measurements have been made beneath the wave zone, although a few have explored the topmost few meters. Furthermore, most measurements have been made in light winds, whereas only a very few have been acquired in strong winds and breaking waves.

The interpretation of surface layer dissipation estimates falls into two broad classes: (i) general agreement with the structure of a classical wall layer as expressed by similarity scaling; (ii) much higher dissipation values than expected from a purely shear-driven wall layer, which are usually attributed to wave breaking. The evidence from individual experiments is at best fragmentary. Given the highly intermittent nature of the small-

* Woods Hole Oceanographic Institution Contribution Number 8509.

Corresponding author address: Dr. E. A. Terray, Dept. AOPE, 217 Bigelow, Woods Hole Oceanographic Institution, Woods Hole, MA 02543.
E-mail: eterray@whoi.edu

scale process of energy dissipation and of one possible source of kinetic energy (wave breaking), and in view of the observational difficulties encountered in making measurements close to the surface of sufficient duration to obtain statistically meaningful results, it is not surprising that the data show a high degree of scatter.

To improve our overall understanding of turbulence near the air–water interface, we undertook an extensive program of field observations in Lake Ontario over three successive autumns (1985–1987). The program was entitled "Water Air Vertical Exchange Studies" (WAVES). The principal players were the National Water Research Institute (the host institute), the Woods Hole Oceanographic Institution, the Finnish Institute of Marine Research, The Johns Hopkins University, and the U.S. Naval Research Laboratory. The experiment produced an extensive set of tower-based data, obtained under a variety of atmospheric forcing conditions. Our purpose in this paper is to present the analysis of dissipation measurements from WAVES, focusing on the vertical distribution of this quantity and its dependence on atmospheric forcing and wave conditions.

2. Review of previous work

The first measurements of dissipation in the ocean were made by Grant et al. (1962) in a tidal channel. This classical work is credited with verifying the Kolmogorov inertial subrange hypothesis. Subsequently, Stewart and Grant (1962) applied the same methods to estimate dissipation near a wind-forced sea surface. They reported nine estimates of ϵ taken over depths of 1–15 m, in the rather restricted wind speed range of 7–10 m s^{-1}, and noted "a rather weak dependence on depth near the surface and the expected increase of ϵ with wave height." When expressed in wall coordinates, the data scatter from about 0.4 to 7 times the expected wall layer value, $u_{*w}^3/\kappa z$ (u_{*w} is the friction velocity in the water, z the depth, and κ von Kármán's constant, 0.4). Because their estimate of the energy flux from the wind exceeded the depth-integrated dissipation by an order of magnitude, they concluded that "almost all wave dissipation is concentrated very near the surface, essentially above the trough line."

Subsequent work (Arsenyev et al. 1975; Dillon et al. 1981; Oakey and Elliott 1982; Jones 1985; Soloviev et al. 1988) found rates of mechanical energy dissipation that were generally consistent with wall layer values. As a result, despite a few reports of substantially higher levels of dissipation (Kitaigorodskii et al. 1983; Gregg 1987; Gargett 1989), the prevailing conceptual model of the ocean surface boundary layer during this period viewed it as an inverted wall layer. Additional evidence, such as the claim that the low-frequency region of the velocity spectrum scales with friction velocity and depth (Jones and Kenney 1977), and reports of logarithmic mean current profiles (Churchill and Csanady 1983), have also been cited to support this view. Although the observations referenced above tend to support the wall layer analogy, they do so for lighter winds or greater depths, whereas more recent studies, designed specifically to explore the very near surface region, have found higher rates of energy dissipation. The latter studies have used a variety of measurement techniques, including tower-based and shipborne current meters of various kinds (Agrawal et al. 1992; Drennan et al. 1996; and this study), and microstructure shear probes mounted both on vertical profilers (Anis and Moum 1992, 1995) and a submarine (Osborn et al. 1992). Significantly, they are in general agreement on the existence of a region adjacent to the surface in which the dissipation rate substantially exceeds wall layer values. Furthermore, the thickness of this layer can be several meters, with one group (Anis and Moum 1992) reporting an order of magnitude enhancement at a depth of 7.5 m.

Although the studies cited above have generally attributed the increased levels of dissipation to wave breaking, the connection has largely been inferential. The strongest observational evidence comes from Osborn et al. (1992), who presented a few cases of high dissipation within bubble clouds. Agrawal et al. (1992) noted that their dissipation estimates (obtained from inertial subrange levels in spectra computed from 13-second velocity records) were highly intermittent and suggested breaking as the source. Theoretical arguments for the role of breaking are based on estimates that the wave field is capable of supplying the required energy flux. In both Drennan et al. (1992b) and this paper, we argue that at high wind speeds the rate of working of the wind on the waves is consistent with the depth-integrated dissipation observed in the water, and hence that most of the energy flux to the waves is delivered into the water column via breaking (this is consistent with measured rates of wave growth). Similar estimates by Melville (1993, 1994), using a slightly different formulation for the wind input, confirm this conclusion. Melville also combined laboratory measurements of the energy flux lost per breaking event with field observations of breaking statistics to make a direct estimate of the energy flux into the upper ocean. The results of this calculation are consistent with the values inferred indirectly from the wind input. Finally, we mention the recent work of Craig and Banner (1995), who used a conventional turbulence closure scheme to calculate the vertical structure of both currents and turbulence close to the surface. They incorporated breaking by specifying a kinetic energy flux at the air–sea interface and accounted for the presence of a free surface permitting the turbulence length scale to take on a nonzero value z_0 there. Although no prescription was given for choosing z_0, by adjusting this parameter over the range 0.1–8 m, Craig and Banner found order of magnitude agreement between their model and the dissipation measurements of Agrawal et

al. (1992), Anis and Moum (1992), and Osborn et al. (1992).

It is clear from this short review that while some features of the observational picture have come into focus, much remains to be resolved. In particular, a reliable experimental delineation of the near-surface structure of turbulence under conditions of active breaking is not yet in hand. Furthermore, presuming that breaking is an important source both of kinetic energy very near the surface and of momentum to the deeper currents, there must be a layer whose scaling is controlled by various characteristics of the wave field, such as wave height and the state of wave development. As one moves away from the surface, the direct effects of breaking diminish, and at some depth we expect wall layer scaling to be recovered. Several important questions that arise from these considerations are: What are the magnitude and vertical distribution of the dissipation in the wave-dominated layer? What are the appropriate scaling variables in each region and how may they be reconciled? We will address these questions in the following sections.

3. The measurements

The choice of experimental site was based on several criteria. Among them were (i) a rigid platform with minimal disturbance to the flow of either air or water near the interface, (ii) good supporting measurements of wave directional properties and meteorological information including wind stress, and (iii) climatology commensurate with a respectable range of wind speeds up to at least 15 m s^{-1}. The air–water field facility of the Canada Centre for Inland Waters (CCIW) provided an ideal site for these measurements. The tower (Fig. 1) is rigidly fixed to the bottom in 12 m of water at the western end of Lake Ontario. It is 1.1 km from the shore so that the prevailing southwesterlies approach it at very short fetch (Fig. 2). This is useful because the resultant strong forcing near the peak tends to produce effects of breaking that are felt well below the trough level. On the other hand, east and northeast winds, which are not uncommon in the fall, may build up substantial waves over the long fetch of the lake (300 km). Waves of 3.5-m significant height have been recorded at the tower and on occasion, much larger waves have swept equipment off the upper deck some six meters above mean water level.

The tower was designed for waves and air–water interaction research, and thus, there is a minimum of interference to flow near the interface. The tower structure disturbs the interfacial layers (from 3 m above the surface to 6 m below) only with four legs of 41-cm diameter and a rotatable mast of ellipsoidal cross section (28.5 cm × 18 cm), on which current meters were mounted. The tower was also equipped with a full set of instrumentation for estimation of the mean environmental conditions, wind stress, and heat flux. A detailed picture of the wave directional properties was provided by an array of six capacitance wave gauges mounted on the north side of the tower (Tsanis and Donelan 1989). Most signals were digitized on the tower and transmitted to the shore station via underwater cable, so that recordings could be made in any weather without the necessity of gaining access to the tower. This capability also permitted us to position various instrument arrays remotely.

During the entire experiment a wide range of conditions were observed including wind speeds up to 17 m s^{-1} (lower wind speeds were generally too variable to permit analysis via Reynolds' averaging techniques); significant wave heights from a few centimeters to 2.5 m; mean current speeds from 2 to 20 cm s^{-1}; and wave development ranging from swell to very young, short-fetch waves. In the analysis and interpretation of our earlier work at the same site (Kitaigorodskii et al. 1983) we realized that, in order to acquire convergent second-order statistics of the velocity field, it was necessary to gather fairly long time series at a particular depth. Consequently, we chose to employ many fixed instruments and to space them out over a suitable depth range.

The data reported here were obtained from three completely different types of current meters: (i) miniature Dragsphere devices, in which the vertical and one horizontal component of velocity are obtained from a measurement of the instantaneous force on a 4-mm sphere attached to the end of a 0.4-mm diameter rod (Donelan and Motycka 1978), (ii) "BASS" acoustic travel-time current meters (Williams 1985), and (iii) a two-axis laser-Doppler velocimeter (Agrawal and Belting 1988).

The Dragspheres were designed to sense velocity fluctuations with wavelengths as small as 2 cm and were sampled at 20 Hz. During 1985 there were three Dragspheres spaced vertically in the upper 4 m; in 1986 and 1987 we deployed two of these devices in the upper 2 m. BASS measures velocities along four directions arranged as orthogonal pairs in orthogonal planes. Each acoustic path is a cylindrical tube having a diameter of approximately 1 cm and a length of 15 cm. Velocity measurements were taken at 20 Hz, averaged internally, and recorded at 5 Hz. In all three years 12 acoustic current meters were installed, spaced at approximately half-meter intervals over the top 6 meters. The Dragspheres and acoustic current meters were mounted in a vertical plane on the west face of the tower, pointing outward on opposite sides of the minor axis of the ellipsoidal mast. The 4-mm spheres and the sensing volume of the acoustic current meters were about 1.5 m on either side of the mast. Forty-five centimeters closer to the mast were two wave staffs, one on either side. The wave staffs were used to estimate the propagation direction of the waves, and this information then used to set the azimuthal orientation of the current meters so as to minimize the flow component across

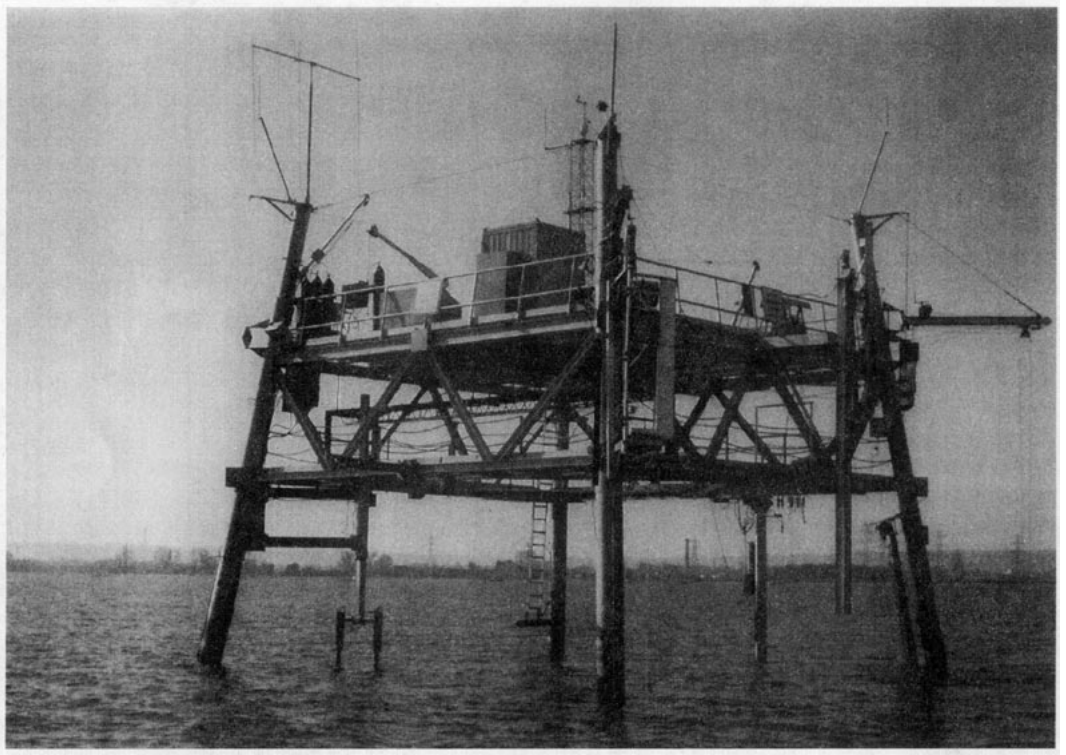

FIG. 1. Photograph of the Canada Centre for Inland Waters research tower, viewed from the northeast, as it was configured during the 1986 field season. The LDV profiler is cantilevered inboard of the southeast leg and the LDV is visible as the inverted U at the bottom of the profiler. The BASS and Dragsphere velocimeters are attached (in this view) to the left- and right-hand sides, respectively, of the rotator mast, which is located in the middle of the west face.

the mast. The laser Doppler velocimeter (LDV) was deployed in the 1986 and 1987 field seasons. It measured the vertical and east–west horizontal velocity components and was sampled at a rate of 128 Hz. The LDV was mounted on a vertical profiler having 1 m of travel. The profiler was separated by 12 m from the ellipsoidal mast holding the other current meters. Time series of 256-s duration were collected at a sequence of four depths separated by 10 cm. Another capacitance wave staff was located at the LDV to provide a local measurement of wave height (this staff was displaced laterally by 30 cm from the sampling volume).

The miniature Dragspheres were difficult and costly to construct and very fragile so that, while we began the experiment with three fully functional instruments, after three seasons we concluded the experiment with a single serviceable one. Their gains were carefully calibrated before and after each field season in the 100-m towing tank at CCIW. Because the force components measured by the Dragsphere depend quadratically on the water velocities, the estimation of both mean and fluctuating velocity components is affected by the quiescent (zero) output of the instrument. This was acquired in the field at the beginning and end of each run (usually 90 minutes long) by remotely positioning a cylindrical sleeve over each instrument. Any significant difference between these pre- and postrun zeros (obtained from 5-min averages) would cause rejection of that dataset. Small differences were removed by subtracting a linear trend through the pre- and postrun zeros. During the 1985 field season, the Dragspheres consistently showed excellent agreement (within 7%) with linear theory (see Drennan et al. 1992a). During the much longer 1987 field season, however, fouling of the Dragspheres due to algal growth caused a gradual increase in drag area. The 1987 Dragsphere data have therefore been recalibrated so as to agree with linear theory in the vicinity of the wave spectral peak.

The acoustic current meters were at a more advanced stage of development and were employed in a greater number. The sensors together with their associated electronics were mounted on two lengths of aluminum channel and were deployed by fastening the channel sections to the rotatable mast at the tower. Pre- and postfield zero offsets, which were measured in the laboratory with the sensors and cables attached to the channels, agreed to within 0.5 cm s^{-1}. The gain of the acoustic current meters depends only on the probe geometry and the speed of sound. Nonetheless, at the end of the experiment we verified both the nominal gain and the cosine response of these sensors in the CCIW 100-m towing tank. Since both the BASS and Drag-

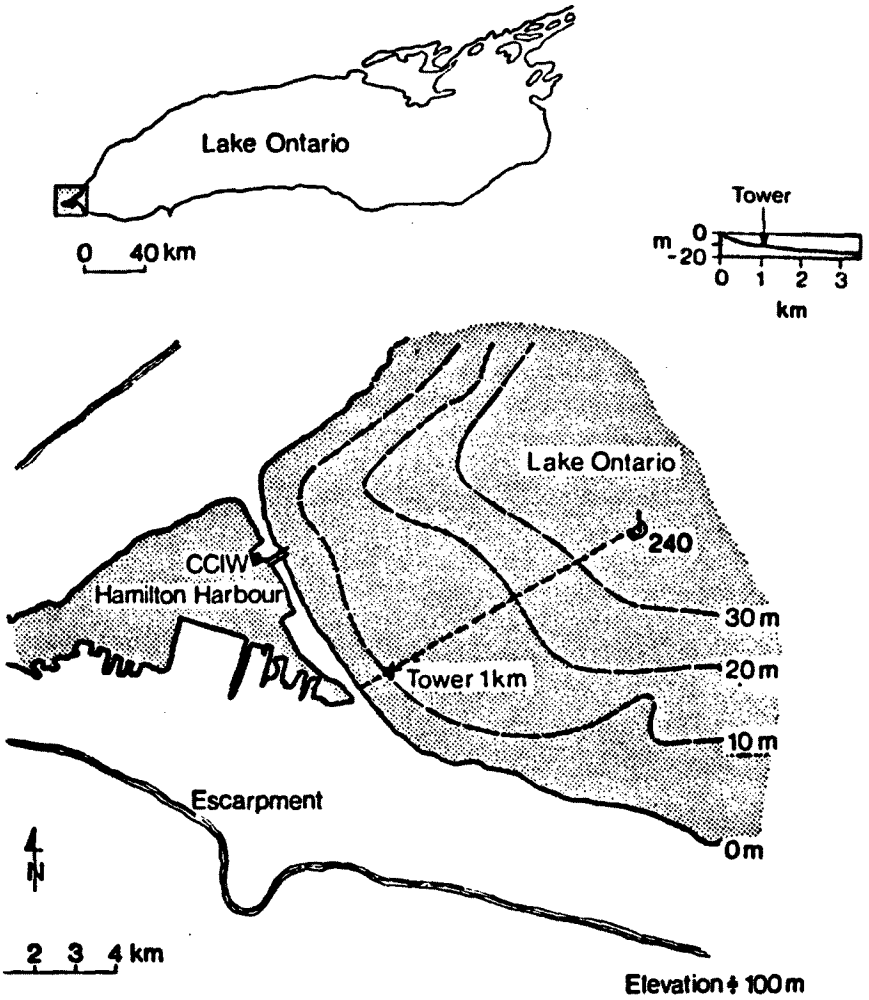

FIG. 2. Map of Lake Ontario showing the site of the WAVES experiment. The tower is located 1.1 km from the western shore on the 12-m isobath.

spheres are in situ instruments, the question of flow disturbance is a critical one for their performance. To investigate this issue we conducted extensive tests of both instruments in the 100-m wind wave flume at CCIW under mechanically produced waves and currents having magnitudes comparable to those observed in the field. The BASS and Dragsphere measurements agreed closely with each other as well as with external measurements of the flow (the wave velocity was deduced from surface displacement using linear theory), even when the rms orbital velocity exceeded the mean current by an order of magnitude. We also conducted runs with the BASS positioned at various distances from a replica of the ellipsoidal mast used to support the instruments in the field. Although a 10% perturbation of the mean flow was measured, there was no measurable increase in spectral levels at frequencies above the wave band.

4. Experimental results

We estimate ϵ from the magnitude of the velocity spectra in the inertial subrange of wavenumbers. In the case of steady advection, the connection between the spatial and the measured frequency spectrum is made via the well-known Taylor "frozen turbulence" hypothesis, which relates the radian frequency and wavenumber via the mean advection, U_d, as $\omega = kU_d$. Then the dissipation rate can be estimated as

$$\epsilon = CU_d^{-1}[S(\omega)\omega^{5/3}]^{3/2}, \qquad (1)$$

where $S(\omega)$ is the one-sided frequency spectrum of velocity evaluated in the range of frequencies exhibiting a $-5/3$ spectral slope. The numerical value of the constant C is either 2.9 or 1.9 depending on whether the direction of the velocity component is in line with or normal to the mean flow, U_d. For the WAVES data

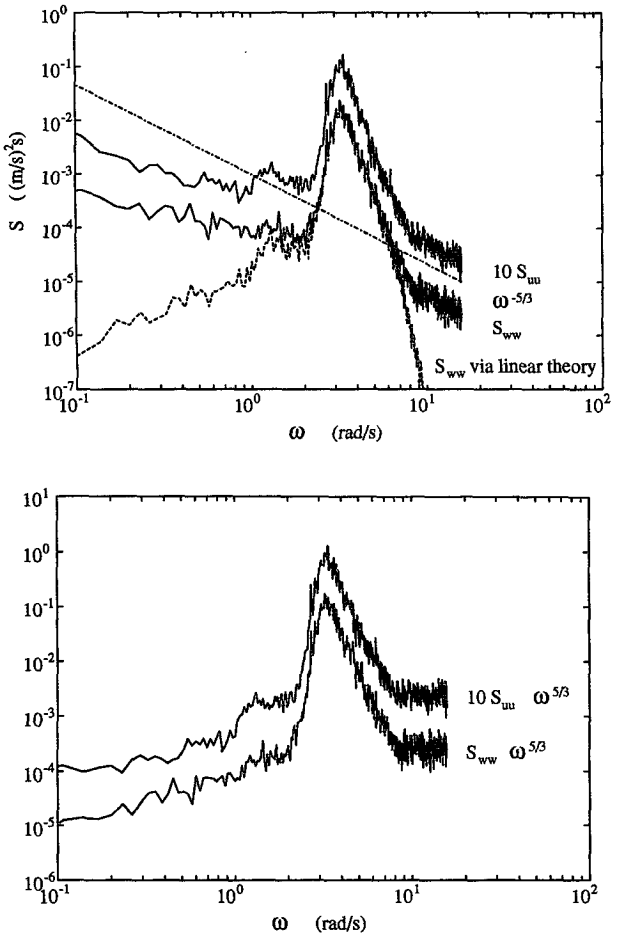

FIG. 3. (a) BASS spectra at 59-cm depth from run 87088 showing horizontal and vertical velocities with $\omega^{-5/3}$ regions. The dashed line is the vertical velocity predicted from the measured wave height using linear theory. (b) Spectra of Fig. 3a multiplied by $\omega^{5/3}$, showing the existence of inertial subranges.

presented here the rms wave velocity exceeded the mean in all cases (their ratio, β, varied from roughly 2 to 15, depending on depth), and therefore we require a generalization of Taylor's hypothesis to unsteady advection. Such an extension has been provided by Lumley and Terray (1983), who analyzed the advection of isotropic turbulence by deep water gravity waves having a narrow directional distribution. They showed that for $\beta > 1$ and frequencies well above the wave peak, Eq. (1) continues to apply with suitable redefinitions of both U_d and C. Taking U_d to be $\sqrt{2}$ times the rms vertical wave velocity, they found $C \approx 2.7$. They further showed that, as a consequence of the circularity of the wave orbits, the apparent horizontal and vertical velocity spectra are equal at high frequencies (in contrast $S_w = \frac{4}{3} S_u$ for rectilinear advection) so that the same constant C applies in both cases. These conclusions were verified in the laboratory by Terray and Bliven (1985) for β in the range 1.7–6. Further support is provided by George et al. (1994), based on hot-film measurements of turbulence in the surf zone. The latter authors compared the predictions of (1) using the prescription of Lumley and Terray to estimates of dissipation based on wavenumber spectra derived from short records over which the wave velocity was large and approximately constant. They reported agreement to within roughly a factor of 2 and attributed the discrepancy to the breakdown of Taylor's hypothesis during the part of the wave cycle in which the horizontal velocity reverses. In contrast, the cases presented here pertain to deep water gravity waves, for which the magnitude of the wave advection remains roughly constant, changing only in direction, so that the results of Lumley and Terray can be applied without modification.

We show typical examples of BASS and Dragsphere spectra in Figs. 3a and 4a. For reference we have also

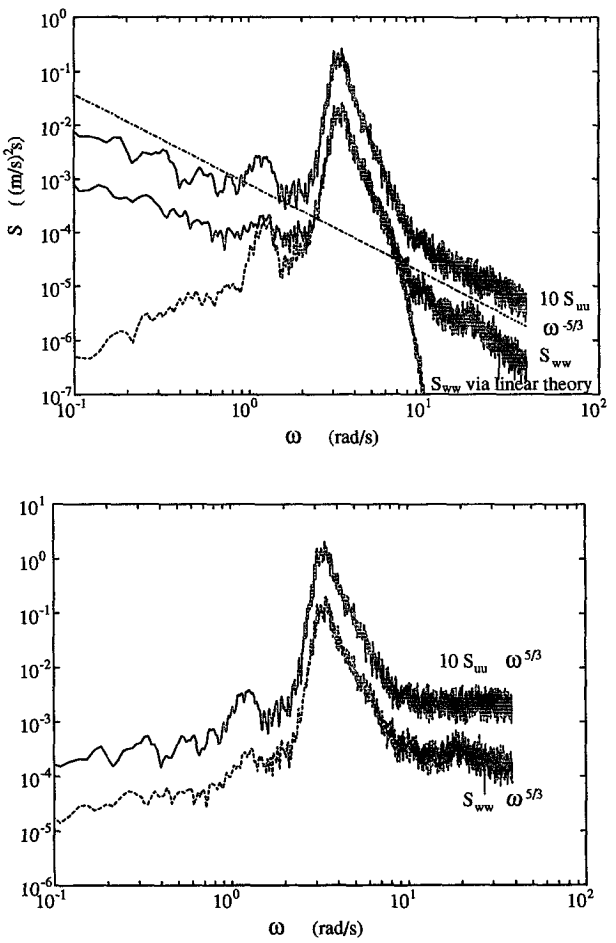

FIG. 4. (a) Dragsphere spectra at 51.5-cm depth from run 87088 showing horizontal and vertical velocities with $\omega^{-5/3}$ regions. The dashed line is the vertical velocity predicted from the measured wave height using linear theory. (b) Spectra of (4a) multiplied by $\omega^{5/3}$, showing the existence of inertial subranges.

TABLE 1. Mean run parameters.

Run	U_{12} (m s^{-1})	U_{12} (deg)	H_s (cm)	T_a (°C)	T_w (°C)	f_p (Hz)	$\bar{c}$ (m s^{-1})	u_{*w} (cm s^{-1})	u_{*a}/c_p	U/c_p
85117	10.43	242.2	26.3	6.81	8.99	0.53	1.45	1.65	0.166	3.54
85159	16.00	235.0	49.0	2.47	6.73	0.41	2.06	2.97	0.231	4.19
85160	12.74	230.1	32.2	−2.86	6.55	0.48	1.71	2.09	0.191	3.92
87025	8.00	243.1	18.4	3.06	7.23	0.64	1.19	1.15	0.139	3.27
87079	7.01	231.7	16.4	14.77	7.06	0.70	0.94	1.01	0.135	3.16
87080	7.71	228.6	17.2	12.76	7.02	0.65	1.07	1.11	0.137	3.21
87082	11.13	238.4	24.9	9.03	6.84	0.53	1.37	1.75	0.177	3.79
87086	12.05	238.7	28.6	7.81	6.76	0.52	1.41	1.96	0.194	4.02
87087	11.41	246.2	28.3	7.89	6.73	0.54	1.48	1.85	0.190	3.95
87088	9.21	266.5	22.7	6.42	6.74	0.56	1.43	1.35	0.144	3.31
87091	11.54	222.0	28.2	7.62	6.58	0.52	1.50	1.85	0.184	3.86
87174	9.30	225.9	20.6	7.39	3.97	0.62	1.25	1.42	0.167	3.69
87184	9.71	245.2	21.4	2.85	4.21	0.62	1.25	1.52	0.179	3.85

plotted the spectrum of vertical wave velocity predicted by applying linear wave theory to the measurements of surface elevation obtained from the collocated wave staffs. The spectra in Figs. 3a and 4a are displayed again in Figs. 3b and 4b, multiplied by $\omega^{5/3}$. The existence at high frequencies of relatively broadband spectral tails having slopes around $-5/3$ is a generic feature of our data. It is clear from the figures that the observed spectral levels in this region lie substantially above the velocity spectrum associated with the waves. We may therefore, without recourse to filtering out the wave-induced motion, treat the spectra at frequencies above the waveband as a reflection of the turbulence properties. Soloviev et al. (1988) have suggested that the very high dissipation rates reported by Kitaigorodskii et al. (1983) are spurious and may be due to limitations in the linear filtration technique used. This is clearly not an issue here, since whatever the drawbacks of linear filtration, its application does not alter the spectra in the $-5/3$ tail well above the wave-dominated central region.

Inasmuch as dissipation estimates are affected by flow disturbances around the velocimeter, particular attention has been paid to identifying and eliminating various sources of flow disturbance. This was a major factor in the design of the tower, and also in the implementation of the experiment. Three criteria were employed in the selection of the data presented in this work. First of all, only west wind cases were used. Not only are the BASS and Dragspheres on the windward side of the tower in these cases but the wind waves are strongly fetch limited, with significant wave heights less than 50 cm and minimal likelihood of turbulence being generated from the legs of the tower. Initially, many east wind cases were analyzed, and for these, typical significant wave heights were around 1–2 m. However, with such large orbital motions, and with the Dragsphere and BASS instruments on the leeward side of the tower, it was thought that the potential for flow disturbance at the measuring sites was high. Hence, the east wind cases were omitted from the final set of runs analyzed here. A second criterion was that the mean current (as measured by BASS) be within ±35° of the normal to the Dragsphere–mast–BASS axis and in the downwind direction. All runs analyzed that were outside this range had a large cross-component of current running from the BASS toward the Dragsphere. For these runs the Dragsphere inertial subrange energy levels were found to be elevated above those of BASS—presumably due to the effects of the mast—and therefore were omitted from the final dataset. We note that the preliminary results presented earlier (Drennan et al. 1992b) were based on the Dragsphere data alone and consequently contained some points that have now been rejected on the basis of the BASS measurements of the mean current direction. The third criterion was simply that the spectrum at frequencies above the waveband be distinguishable from the noise floor. For the purpose of estimating dissipation, the effect of this was to limit the useful measurement range to the topmost 2 m. The degradation of the spectral signal to noise ratio is apparent in Fig. 7 from the increased scatter of the measurements toward the bottom of this range of depths. A summary of environmental parameters for runs satisfying these three criteria is given in Table 1.

The dissipation estimates from the BASS and Dragspheres were obtained from 90-min records using Eq. (1), averaged over a bandwidth of several hertz (the actual bandwidth varied with each instrument and from run to run), and assuming a spectral slope of exactly $-5/3$. Based on the statistics of the spectral estimates, the standard error in dissipation is approximately 1%. The Dragsphere has a spherical sampling volume, approximately 0.4 cm in diameter, and was sampled at 20 Hz. Velocity spectra obtained from it typically have a well-developed $\omega^{-5/3}$ region spanning a decade or more in frequency. Although BASS was sampled at 20 Hz, the output was averaged and recorded at the lower rate

of 5 Hz, resulting in a smaller range of frequencies that could be used to determine the spectral level. Although the actual spectral slopes were variable around $-5/3$ (Figs. 3a and 4a are typical examples), in general the deviations were small. We offer two consistency checks on our fitting procedure. First, estimates of ϵ using both the horizontal and vertical velocity spectra from the BASS and Dragsphere are compared in Fig. 5. The range of ϵ covers $2\frac{1}{2}$ decades and exhibits good agreement between the estimates from either component. Second, it is apparent (from Fig. 7) that the agreement between the BASS and Dragsphere is quite good, particularly in view of the fact that their sensing volumes were separated by roughly 3 m in the crosswind direction.

The LDV measurements were acquired as repeated 256-s records at depths of 20, 30, 40, and 50 cm so that the data listed in Table 2 represent an observation period of slightly less than 20 minutes at each depth. Although measurements from the three lower depths were essentially continuous, the dropout rate at 20 cm was roughly 10% (presumably because of the occasional interruption of the beams during passage of the higher waves). Simulation has indicated that this level of dropout can significantly affect the spectrum at high frequencies, and for this reason we have excluded the 20-cm observations from the data reported here. An estimate of dissipation was obtained for each 256-s record from the level of the vertical velocity spectrum in the inertial subrange. The four individual estimates of dissipation at each depth were then averaged to obtain the result given in Table 2. The standard error of the average of the four estimates is roughly 20%. While some individual 256-s records yield dissipation rates in agreement with those observed by the Dragspheres and BASS, the averaged LDV results lie below the other two sensors (although they have roughly the same logarithmic slope). We have considered and ruled out a large number of explanations for this discrepancy, and its cause must be regarded as unknown.

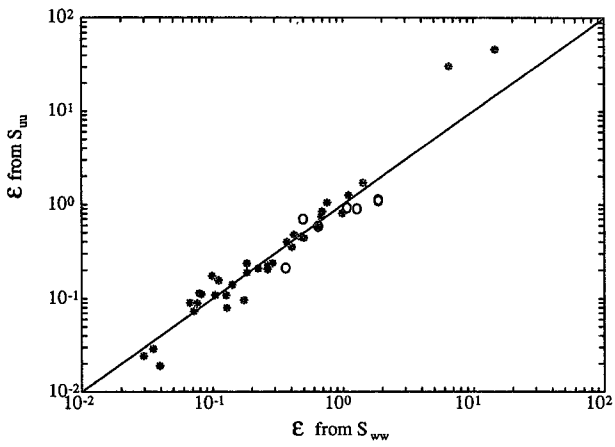

FIG. 5. Turbulent kinetic dissipation rate ϵ from horizontal versus ϵ from vertical velocity spectra using frequencies above the waveband. Points marked * were measured by BASS; ∘ are Dragsphere data.

TABLE 2. Dissipation values. Bass and Dragsphere estimates are based on continuous 90-min records. Corresponding LDV results at each depth are averages over four 256-s records taken at different times during the 90-minute period.

Run	Instrument	z (cm)	e_u (cm^3 s^{-2})	e_w (cm^3 s^{-2})	U_a (cm s^{-1})
85117	DragSph	140.0	0.21	0.36	6.08
85159	DragSph	174.0	0.90	1.27	13.78
85160	DragSph	100.0	0.59	0.64	13.56
87025	DragSph	49.6	0.92	1.06	10.51
87079	BASS	25.1	1.05	0.76	13.18
87079	BASS	65.1	0.19	0.18	6.25
87079	BASS	105.1	0.17	0.10	4.27
87079	BASS	155.1	0.09	0.08	3.51
87079	BASS	215.1	0.09	0.07	2.94
87080	BASS	65.0	0.21	0.22	7.91
87080	BASS	105.0	0.16	0.11	4.71
87080	BASS	155.0	0.11	0.08	3.37
87080	BASS	215.0	0.12	0.08	2.73
87082	BASS	60.6	0.59	0.64	12.88
87082	BASS	100.6	0.21	0.26	7.65
87082	BASS	150.6	0.11	0.13	4.40
87082	BASS	210.6	0.07	0.07	2.56
87086	BASS	15.3	46.51	14.66	35.20
87086	BASS	55.3	1.70	1.43	20.83
87086	BASS	95.3	0.81	0.98	13.48
87086	BASS	145.3	0.40	0.37	9.14
87086	BASS	205.3	0.08	0.13	5.33
87087	DragSph	51.6	0.70	0.49	18.08
87087	BASS	19.2	30.68	6.51	31.86
87087	BASS	59.2	1.26	1.11	18.38
87087	BASS	99.2	0.56	0.65	11.44
87087	BASS	149.2	0.24	0.18	7.89
87087	BASS	209.2	0.02	0.04	4.55
87088	DragSph	51.5	1.10	1.85	14.56
87088	BASS	59.1	0.45	0.48	12.98
87088	BASS	99.1	0.10	0.17	7.35
87088	BASS	149.1	0.03	0.04	4.12
87091	BASS	59.9	0.74	0.68	17.79
87091	BASS	99.9	0.35	0.41	11.44
87091	BASS	149.9	0.11	0.10	7.07
87091	BASS	209.9	0.02	0.03	4.19
87091	LDV	30.0	—	0.54	21.98
87091	LDV	40.0	—	0.33	19.08
87091	LDV	50.0	—	0.19	15.77
87174	DragSph	61.9	1.41	—	10.29
87184	DragSph	62.5	1.12	1.85	10.42

5. Dissipation rate scaling

Soloviev et al. (1988) have argued that the appropriate physical variables for describing the scaling of ϵ in the upper ocean are the friction velocity u_{*w}, depth z, and gravitational acceleration g. The wind action is reflected in u_{*w} and g is intended to account for the presence of surface gravity waves at the interface. They continue their development by using dimensional analysis to suggest that $\epsilon z/u_{*w}^3$ should be a function solely of gz/u_{*w}^2.

This approach embodies several limitations. First, Soloviev et al. have restricted their discussion to the case of full development. This results in their use of u_{*w}^2/g, which is proportional to the wave height at full development, as a length scale. However, it is likely that this scale may be a substantial overestimate when the waves are not fully developed. Second, the apparent agreement with wall layer scaling cited by Soloviev et al. requires that the layer in which wave breaking dominates lies above their observed depths. They justify this by referring to Csanady (1984) and conclude that all measurements cited, including those of Kitaigorodskii et al. (and of this study), are made below the wave breaking zone. However, Csanady's estimates of the depth of the well-mixed layer due to breaking were based on observations of drifters in relatively calm seas disturbed primarily by breaking wavelets. Furthermore, the full dataset he presents does not yield a single breaking zone depth but, in fact, a range of depths covering almost two orders of magnitude, from $zg/u_{*w}^2 \approx 1.3 \times 10^{-5}$ to 1.7×10^{-7}. Clearly, a well-defined transition depth does not arise using the Soloviev et al. depth coordinate. A final objection, pointed out in Agrawal et al. (1992) is that the WAVES data, involving strong forcing and underdeveloped waves, do not collapse under the Soloviev et al. scaling. We believe that all of these considerations point strongly to the need to take explicit account of wave development in the parameterization of upper-layer turbulence.

On the other hand, whereas Kitaigorodskii et al. (1983), Agrawal et al. (1992), and others have found enhanced dissipation close to the surface, it is clear from the data compiled by Soloviev et al. that sufficiently far from the air–sea interface the dissipation rate is similar to that observed in shear flows over solid boundaries. Our objective here is to propose a framework that encompasses these, apparently dissimilar, observations and gives a quantitative measure to the notion of "sufficiently far."

The scaling we propose below is based on two physical hypotheses. First, we assume that at high wind speeds wave breaking is the principal source of turbulent kinetic energy in the near-surface layer and second that the thickness of the layer in which the energy is initially deposited (i.e., the region that is directly stirred by the breaking) is proportional to wave height. These two propositions, although not unique, are consistent with our data and lead to specific predictions concerning the vertical structure of dissipation close to the surface that are amenable to experimental verification.

The justification for the first hypothesis lies in the observation that when the surface is aerodynamically rough (this condition depends on wave development but corresponds to wind speeds above roughly 8 m s^{-1}) the energy and momentum fluxes from the wind to the water are transmitted by normal stresses on the roughness elements themselves (i.e., to the waves). Because the waves are known to retain only a small fraction of these fluxes (Hasselmann et al. 1973; Donelan 1978; Mitsuyasu 1985), it follows that, regardless of the spectral distribution of wave dissipation, the vertically integrated dissipation rate in the water will be approximately equal to the mean energy flux from the wind to the waves. Given the unsatisfactory state of our present understanding of wave dissipation (Hasselmann 1974; Phillips 1985; Donelan and Pierson 1987), this presents an essential simplification and is central to the discussion that follows.

Support for our second hypothesis is more tenuous. It is known, based on the laboratory results of Rapp and Melville (1990) concerning the breaking of focused wave packets, that the immediate production of turbulence extends to depths on the order of the height of the breaking wave, that is, the maximum superposed height of the group. Although breaking over a wind-generated spectrum of waves is undoubtedly more complex (for example, fluctuations in wind forcing may be dissipated quasi locally in wavenumber by short waves that are strongly coupled to the wind), the breaking of waves near the peak of the spectrum (which are generally weakly coupled to the wind) almost certainly involves superposition and hence should be closely related to the mechanics elucidated by Rapp and Melville. Since the energy and momentum fluxes per breaking event increase with increasing wavelength, the maximum depth of direct injection is therefore likely to be determined by the breaking of waves around the peak of the spectrum (the direct stirring by shorter breaking waves will be nested within the dominant scale), and hence we expect the significant height of the wind waves, H_s, to provide a suitable choice of vertical scale.

We begin by defining a normalized wind input, F, such that $\rho_w F$ is the energy flux from the wind to waves. Note that this normalization is in keeping with the usual definition of ϵ as the rate of energy dissipation per unit mass. In deep water, we expect the dissipation rate to be a function of z, u_*, H_s, c_p, k_p, and F. (For the unstratified case under consideration here the air and water densities can enter only as their ratio whose principal role is to relate the corresponding friction velocities; consequently, we will henceforth drop explicit reference to density and use either friction velocity interchangeably, distinguishing them when necessary by means of the subscripts "a" and "w.") Note also that, while we have not listed the gravitational acceleration g explicitly, it is implicit in the dispersion relation that links k_p and c_p. Following our previous discussion, we choose to nondimensionalize the dissipation rate by F and H_s. Based on dimensional analysis, the normalized dissipation must then be a function of four dimensionless variables, which we take to be the ratios z/H_s, c_p/u_*, $F/u_*^2 c_p$, and $k_p H_s$. In the case of fetch-limited waves it is conventional practice to parameterize the state of wave development in terms of wave age, c_p/u_* (Donelan et al. 1985). Accordingly, we drop the

last two variables, wave steepness and normalized energy flux, since they can be expressed as functions of wave age. Note that this argument also applies to other dimensionless combinations of wave variables, such as the normalized spectral bandwidth, etc. Although, strictly speaking, a description purely in terms of wave age must be an approximate one, we believe that it captures the main features of the development of the wave spectrum that are important in determining the energy flux through the air–sea interface.

Based on the above arguments, a scaling law for upper-layer dissipation under breaking wave conditions can be written as

$$\frac{\epsilon H_s}{F} = f(z/H_s, c_p/u_{*a}), \tag{2a}$$

where f is a function to be determined from the data, and we have used the conventional definition of wave age in terms of the air-side friction velocity. Although this expression depends on two variables, the WAVES data suggest that when scaled in this way, there is a range of depths near the surface over which the nondimensional dissipation rate does not depend explicitly on wave age. Therefore we conjecture that there is an intermediate depth range over which

$$\frac{\epsilon H_s}{F} \to f(z/H_s). \tag{2b}$$

It is important to note that Eq. (2b) can only be valid close to the surface, since a dependence on c_p/u_{*a} is required to recover the observed wall layer scaling (i.e., $\epsilon z/u_{*w}^3 = \text{const}$) at greater depths.

Before proceeding further, we need to determine the dependence of the wind input on wave age. The rate of energy input to the waves from the wind, F, is defined as the integral of the growth rate, β, over the wave spectrum, where β is the e-folding scale for the temporal growth of wave energy in the absence of nonlinear interactions and dissipation. Then

$$F = g \int \frac{\partial S_\eta}{\partial t} d\omega d\theta = g \int \beta S_\eta d\omega d\theta, \tag{3}$$

where $S_\eta(\omega, \theta)$ is the frequency–direction spectrum of the waves. There is general agreement, based on both theory (Jeffreys 1924, 1925; Miles 1957) and experiment (Plant 1982), that β is quadratic in either the wind speed or friction velocity. We use a formulation due to Donelan and Pierson (1987) that relates β at each frequency to the wind speed as

$$\frac{\beta}{\omega} = 0.194 \frac{\rho_a}{\rho_w} \left(\frac{U_{\pi/k} \cos\theta}{c(k)} - 1 \right) \left| \frac{U_{\pi/k} \cos\theta}{c(k)} - 1 \right|, \tag{4}$$

where for a wave component of wavenumber $\vec{k}$, having phase speed $c(k)$, both the magnitude, U, and direction, θ, of the wind are evaluated at a reference height of π/k (i.e., at one-half the wavelength).

We can define an "effective phase speed", $\bar{c}$, related to wind input by parameterizing F in terms of this speed and the wind stress τ_a as

$$F \equiv \tau_a \bar{c}/\rho_w \approx u_{*w}^2 \bar{c}, \tag{5}$$

where we have made use of the approximate equality between the wind stress and the surface value of the turbulent stress in the water, $\tau_a \equiv \rho_a u_{*a}^2 \approx \rho_w u_{*w}^2$ (the latter relation follows from our assumption that the entire wind stress is supported by the waves and that only a few percent of the applied stress is necessary to account for the observed growth of the waves with fetch).

As defined in (5), $\bar{c}$ is an integral measure of the characteristic velocity associated with the energy flux and arises from contributions over the entire spectrum. At one extreme of wave development, typically realized in laboratories, it approaches the peak wave velocity, while at the other, near full development, it is of the order of the friction velocity u_{*a}. We have computed $\bar{c}$ using Eqs. (3), (4), and (5) for a wide variety of observed wave spectra drawn from both the WAM database (Kahma and Calkoen 1992) and this experiment. The results, normalized by the phase speed at the peak of the wave spectrum, are shown in Fig. 6 as a function of inverse wave age, u_{*a}/c_p. In order to calculate the integral in (3), the observed spectra were extended to frequencies beyond $3.5\omega_p$ by appending an ω^{-5} tail (Banner 1990). Since most of the WAM database does not include measurements of wave direction, we carried out the angular integrations in (3) using the parametric form of the directional distribution, $\text{sech}^2(\alpha\theta)$, proposed by Donelan et al. (1985). The dominant contributions to (3) come from the rear face of the spectrum where the directional spread of the waves is large (in this region $\alpha \approx 1.2$ and the rms directional spread is roughly 40 degs). As a result, our calculation is not especially sensitive to the choice of angular distribution. Friction velocities in the air were calculated using the relation

$$u_{*a} = \kappa \frac{U_{10}}{\ln(10/z_0)}. \tag{6}$$

The roughness length z_0, needed in (6), was computed from an empirical regression based on previous meteorological observations taken at the WAVES site (Donelan 1990):

$$\frac{z_0}{H_s} = 1.38 \times 10^{-4} \left(\frac{U_{10}}{c_p} \right)^{2.66}. \tag{7}$$

Figure 6 shows that $\bar{c}$ is roughly 10% of c_p near full development but that it rises quickly to a fairly constant value of 50% for u_{*a}/c_p larger than 0.075. Although Fig. 6 includes the entire range of wave development encountered during WAVES, the subset used here to determine the dissipation rate all have $\bar{c}/c_p$ approximately 0.5.

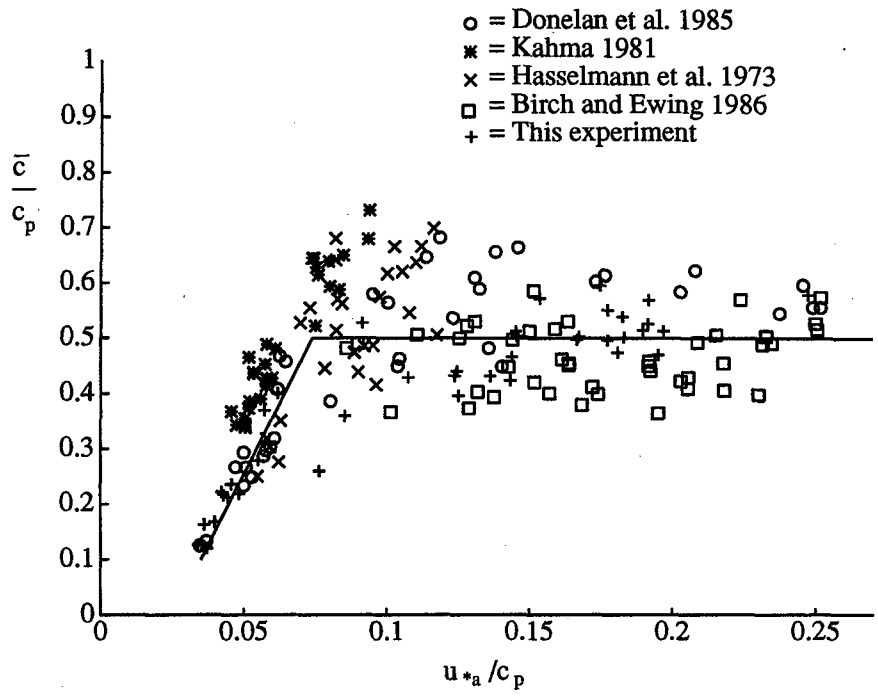

FIG. 6. The ratio $\bar{c}/c_p$ versus inverse wave age, u_{*a}/c_p, where $\rho_a u_{*a}^2 \bar{c}$ is the energy flux from the wind to the waves.

As a consistency check, we repeated the above calculation using the form for β given by Plant (1982):

$$\frac{\beta}{\omega} = 0.04\left(\frac{u_{*a}}{c(k)}\right)^2 \cos\theta. \tag{8}$$

The results for $\bar{c}/c_p$ closely follow those shown in Fig. 6, although they are roughly 20% higher. This is not unexpected, however, since in Plant's formulation the coupling of the wind to waves near the spectral peak is greater than in (4), resulting in a somewhat higher estimate of $\bar{c}$.

Figure 7 shows the WAVES dissipation values normalized as in (2) by significant height H_s and wind input F plotted against nondimensional depth z/H_s. For the data under consideration, we have estimated F from (3) and computed u_{*a} from Eqs. (6) and (7). The data plotted in Fig. 7 span the range $4.3 < c_p/u_{*a} < 7.4$. Over most of the depths shown they are reasonably tightly clustered and do not show a systematic dependence on wave age. A linear regression on logarithmic variables yields a slope of approximately -1.9. The residuals are independent of c_p/u_{*a} so that, within the uncertainty of the fit, the regression may be expressed as

$$\frac{\epsilon H_s}{u_{*w}^2 \bar{c}} = 0.3(z/H_s)^{-2}. \tag{9}$$

Both the linear regression and (9) appear in Fig. 7—the two are barely distinguishable.

6. The vertical distribution of dissipation

The form of the dissipation rate given by (9) is valid over a range of depths determined by the twin requirements that the vertically integrated dissipation matches the wind input and that, below some depth, the dissipation rate relaxes to the conventional wall layer result, $u_{*w}^3/\kappa z$. This latter condition enforces consistency with previous observations of wall layer behavior at sufficient depth (e.g., Soloviev et al. 1988).

It is useful at this point to review briefly the assumptions underlying our approach. We have postulated that the principal source of turbulent kinetic energy is wave breaking and that the breaking directly injects energy to a depth, z_b, which is of the order of a wave height. We further assume that the dissipation rate between the surface and z_b has a constant value, ϵ_b, which can be estimated by evaluating (9) at z_b. We note that a similar idea was proposed by Kitaigorodskii (1984) in connection with a model for gas transfer. The energy in this "breaking layer" is transported downward and simultaneously dissipated. However, wave breaking also transfers horizontal momentum to the near-surface currents so that, viewed on a large enough scale, the flow must be vertically sheared (although the shear may be small close to the surface where turbu-

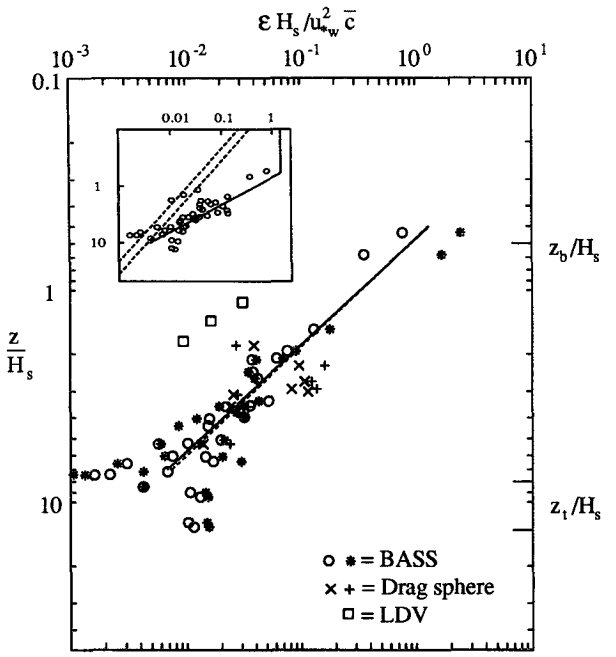

FIG. 7. The normalized dissipation rate, $\epsilon H_s/u_{*w}^2\bar{c}$, versus dimensionless depth, z/H_s; O and × represent data calculated from horizontal velocity fluctuations S_{uu}; the remaining points are via S_{ww}; z_b and z_t (on the right-hand ordinate) are the length scales of the breaking zone and the transition depth to wall layer, with the range of the latter due to variations in $\bar{c}/u_*$ in the dataset. The dashed line is the regression line to the dataset in the range covered by the line. The solid line is Eq. (9). The inset shows the data (only one set of points per instrument, all denoted with O), the wall layer scaling for the data (dashed), and the proposed vertical structure: constant dissipation down to z_b, $(z/H_s)^{-2}$ scaling to z_t with a transition to wall layer scaling at greater depths. The two (dashed) wall layer lines show the possible range for the data in these coordinates.

lence levels are high). Hence, we expect that there is a transition depth z_t below which local shear production dominates the infusion of kinetic energy of breaking from above, and the turbulence energetics resemble those of flows over a rigid boundary.

As discussed previously, the vertical integral of the dissipation in the water must balance the wind input, $u_{*w}^2\bar{c}$. The net dissipation consists of three terms: 1) the integral of the wall layer dissipation $u_{*w}^3/\kappa z$ from the bottom (in the present case at 12 m) to z_t (if a thermocline is present, the lower limit should be taken as the base of the mixed layer); 2) the contribution of (9) from z_t to z_b; and finally 3) the integral of the constant dissipation, ϵ_b, from z_b to the surface. It is readily verified that the integral of the wall layer dissipation can be neglected with respect to the other two terms. It is interesting to note that because of the z^{-2} depth dependence in (9) the magnitudes of the two remaining contributions are nearly the same [they are equal up to terms of order $O(z_b/z_t)$]. The integral constraint leads to the following approximate expression for the "breaking depth" z_b

$$z_b/H_s \approx 0.6, \tag{10}$$

which is consistent with our original physical assumption that a length scale related to the significant wave height is *imposed* by the mechanics of breaking.

Matching (9) to the conventional wall layer result, we obtain an expression for the transition depth z_t:

$$z_t/H_s = 0.3\kappa\bar{c}/u_{*w} \approx 3.6(\bar{c}/u_{*a}), \tag{11}$$

where we have taken $\rho_w/\rho_a = 880$. Combining (10) and (11) gives

$$\frac{z_t}{z_b} = \frac{\kappa}{2}\left(\frac{\bar{c}}{u_{*w}}\right) \approx 6\frac{\bar{c}}{u_{*a}}. \tag{12}$$

The values of z_b/H_s and z_t/H_s as defined in (10) and (11) are indicated in Fig. 7, with the range of z_t/H_s corresponding to that of the current dataset. For the young, fetch-limited waves reported here, $\bar{c} \approx 0.5c_p$, so that the right-hand side of (12) is proportional to the wave age. It is of interest to see how the thickness of the transition layer z_t/H_s varies over a wider range of wave development. To address this question, we computed $\bar{c}/u_{*a}$ as a function of wave age, c_p/u_{*a}, using both the WAM database (Kahma and Calkoen 1992) and the full set of WAVES data. The results are displayed in Fig. 8 and show that $\bar{c}/u_{*a}$ at first increases in proportion to wave age, reaches a maximum of roughly 7–8, and then decreases by a factor of 2 or more (relative to the maximum) as full development is approached. Combined with (11), these results imply that the depth of the crossover from a z^{-2} to z^{-1} behavior may be as large as $25H_s$ at some intermediate stage of wave development. For the dissipation values shown in Fig. 7, $2.3 < \bar{c}/u_{*a} < 3.6$, giving a transition depth in the range $8.3 < z_t/H_s < 13$, or (from Table 1), $1.8 < z_t < 4$ m.

The ratio of dissipation in the intermediate (z^{-2}) layer to the conventional wall layer estimate is given by

$$\frac{\epsilon\kappa z}{u_{*w}^3} = \frac{z_t}{z}. \tag{13}$$

Thus, our dissipation estimates rise from the conventional estimates at z_t (by definition) to a value z_t/z_b times the conventional estimates at the base of the layer of direct injection of turbulence by breaking. This, from (12) and Fig. 8, may be as large as 45 times the wall layer estimate.

7. Discussion

The scaling on significant height H_s and wind input F introduced in Eqs. (2a,b) is motivated by a physical picture in which the energy flux from wave breaking is initially deposited into a relatively thin wave-stirred layer adjacent to the surface. Following Rapp and Melville (1990), we have supposed that the thickness of

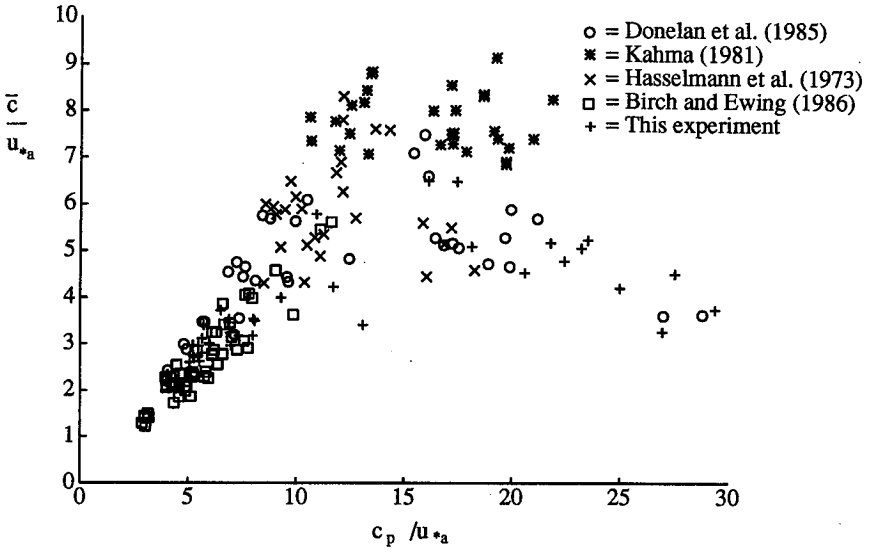

FIG. 8. The ratio $\bar{c}/u_{*a}$ versus wave age, c_p/u_{*a}.

this layer, z_b, is determined by the mechanics of the breaking process itself and is proportional to the significant height of the actively wind-driven waves. Below this there is an intermediate region into which kinetic energy is transported from above by turbulence and in which the dissipation rate decays with depth as z^{-2}. This layer eventually merges into a classical wall layer at the transition depth z_t, below which the dissipation rate decays as z^{-1}. A schematic illustration of this behavior appears in the inset to Fig. 7. Although we have shown in the preceding sections that the scenario described above provides a consistent description of dissipation beneath the fetch-limited, strongly forced waves observed during WAVES, it is of interest to ask whether our principal results, embodied in (9)–(11), can be reliably extended to any degree of wave development. Although it remains for future experiments to provide a definitive answer to this question, some insight can be obtained by critically examining the premises underlying the arguments of the preceding sections.

First, we consider the magnitude of the dissipation (i.e., its vertically integrated value). We have assumed from the start that the energy flux to the waves can be used as a surrogate for the net dissipation in the water. As mentioned earlier, this requires that we can neglect both the direct viscous stresses on the surface and the production of kinetic energy in the water by shear currents. The latter assumption has been verified a posteriori from the observed dissipation. To address the former, we consider the conventional estimate of the energy flux into the upper layer, $\tau_s U_d$. This expression neglects breaking and assumes that the energy flux arises from the direct action of shear stresses τ_s on the surface current U_d. Based on Wu's (1975) estimate, $U_d \approx u_{*a}/2$, the rate of working on the surface current is bounded by $\rho_a u_{*a}^3/2$. Computing F from Eq. (5), we find that the energy flux from the wind to the waves, and hence the flux available to currents via breaking, is enhanced relative to the conventional estimate by a factor of $2\bar{c}/u_{*a}$. As shown in Fig. 8, this ratio is a function of wave development. It is proportional to wave age, c_p/u_{*a}, for immature waves, reaches a maximum of roughly 16 at $c_p/u_{*a} \approx 15$, and then decreases to around 3 near full development. Thus, for wave age of about 15 (corresponding to $U_{10}/c_p \approx 2$), the energy flux from breaking exceeds the conventional estimate by a factor of roughly 16. The discrepancy is less for both younger and older waves. Considering for the moment the case of a developing sea under a constant wind, c_p increases monotonically to its asymptote, while $\bar{c}$ first increases and then decreases as the waves mature from very young to fully developed. This behavior reflects a change in the net wind forcing and arises because in very young seas ($c_p/u_{*a} \leqslant 15$) the peak of the spectrum is enhanced (Donelan et al. 1985) and much of the energy input goes to the steep waves at the peak. As the waves become more mature, the enhancement diminishes until the largest waves are less steep than those in the equilibrium range and support less of the stress and energy flux. Thus, in the early stages of development $\bar{c}$ tracks c_p, whereas in the later stages of development the net energy flux decreases due to the reduction of the peak enhancement.

The distribution of the dissipation with depth is characterized by the breaking and transition depths, z_b and z_t. Since the bandwidth of the transition layer, z_t/z_b, is simply $6\bar{c}/u_{*a}$, the discussion above concerning the dependence of the normalized energy flux on wave age applies to this quantity as well. Our estimate of z_b is

based on the assumption that the dissipation rate in the breaking layer is roughly constant. This leads to the conclusion that approximately half the total dissipation in the water occurs within z_b of the surface and yields the estimate $z_b \approx 0.6H_s$. Although this is slightly outside the depth range of our observations (see the inset in Fig. 7), a substantially larger value would be observable. Although we have assumed that the dissipation above z_b is constant, our conclusions are not significantly affected as long as z_b marks the beginning of a roll-off of the dissipation toward its surface value.

Recall that our basic conjecture in obtaining Eq. (2b) is that an intermediate range of depths exists over which the dependence of the dissipation rate on wave age is implicit through the wave-related scaling variables H_s and F. Whereas the importance of the energy flux F in the scaling of dissipation seems to us clear on physical grounds, the choice of a length scale is more problematic, although it must be a wave-related scale characterizing breaking. For example, Drennan et al. (1992b) suggested the use of the wavenumber at the peak of the wind sea, k_p. Note that the significant slope, $k_pH_s \approx 0.9(u_{*a}/c_p)^{0.5}$, depends only weakly on wave age (Maat et al. 1991). Therefore, because the results presented here span the narrow range of wave age $4.3 < c_p/u_{*a} < 7.4$, they cannot be used to distinguish between H_s and k_p as the better choice of scaling variable, and it remains for future experiments to provide an unambiguous determination of the correct length scale (see also Drennan et al. 1996).

Our conclusion that the thickness z_t of the enhanced dissipation layer depends on wave age is consistent with the measurements of Osborn et al. (1992), which were taken under more fully developed wave conditions. Their Fig. 9b shows a dissipation profile exceeding wall layer values by nearly an order of magnitude close to the surface, relaxing to levels consistent with a wall layer below depths of 8–10 m. Estimating their wave age as $c_p/u_{*a} \approx 30$, we find from our Fig. 8 that $\bar{c}/u_{*a} \approx 3$. Using their estimated significant wave height of 1 m, we conclude $z_t \approx 10$ m. Furthermore, from Eq. (13) the ratio of breaking to wall layer dissipation is simply z_t/z, so we expect in this case an enhancement of the dissipation by roughly a factor of 10 at a depth of 1 m. Both of these results are consistent with Osborn et al.

It is of interest to ask whether our conclusions are consistent with what is known about the ability of the wave field to deliver energy fluxes of the required magnitude via breaking. This issue has been addressed recently by Melville (1993, 1994). Based on previous work by Thorpe (1992), Melville suggests that the energy flux into the upper layer from breaking can be estimated as $E_w \approx 4.3 \times 10^{-6}\, \rho_w U_{10}^3 (c_b/c_p)^5$, where c_b is the phase speed of the breaking waves. Equating this to our expression for the wind input, $\tau_a \bar{c}$, we find that $c_b/\bar{c} \approx 0.4(c_p/\bar{c})(\bar{c}/u_{*a})^{0.2}$. Using the results given in Figs. 6 and 8 for the dependence of the ratios $\bar{c}/c_p$ and $\bar{c}/u_{*a}$ on wave age, we find that $1 < c_b/\bar{c} < 5$ for $2 < c_p/u_{*a} < 30$. For wave ages less than 12 or so, $c_b/\bar{c} \approx 1$, suggesting that for young waves the dissipation is quasi-local to the wind input. As full development is approached, $c_b \gg \bar{c}$, indicating that while the direct wind forcing remains relatively localized at high wavenumbers, the waves participating in breaking extend over a much wider bandwidth including most, if not all, of the rear face of the spectrum.

Finally, we discuss the work of Craig and Banner (1994), which is the first systematic attempt to apply a turbulence model to the description of mixing in the near-surface region. Their model, which is based on a conventional low-order closure, includes equations for momentum and kinetic energy, and incorporates the effect of wave breaking via an enhanced flux of kinetic energy at the air–sea interface together with the specification of a turbulence length scale l. They choose $l = \kappa(z_0 + z)$, where $z_0 > 0$ is a "roughness length" (note we are using the convention, which is opposite to Craig and Banner's, that the fluid occupies $z > 0$). Over the region $z_0 \leq z \leq 6z_0$, their model predicts that the dissipation rate decays as

$$\frac{\epsilon z_0}{\alpha u_{*w}^3} = 2.4(1 + z/z_0)^{-3.4}, \qquad (14)$$

where they have defined αu_{*w}^3 to be the surface value of the kinetic energy flux. The form of ϵ in (14) reflects a dominant balance close to the surface between turbulent transport and dissipation. Written in this way, Craig and Banner's result is consistent with our conjecture that, suitably scaled, the dissipation rate is a function solely of the dimensionless depth. If we identify $z_0 \sim H_s$ and estimate the kinetic energy flux at the surface by the wind input (so that $\alpha = \bar{c}/u_{*w}$), then over the transition layer, Eq. (14) is in good empirical agreement with our data and hence with Eq. (9). That this should be so is not immediately apparent because of the difference in exponents between (9) and (14). It comes about due to the slow approach of the function $(1 + z/z_0)^{-3.4}$ to its asymptote, $(z/z_0)^{-3.4}$, when plotted as a function of depth. The latter is not fully reached until z/z_0 exceeds 20 or so, a depth at which shear production has significantly modified the profile. Since the thickness of the transition layer in Craig and Banner's model is roughly $6z_0$, the dissipation rate in this layer decays more slowly than its asymptotic limit (i.e., closer to z^{-2})—behavior that is preserved in the full model, as is evident from their Fig. 7.

8. Conclusions

We have explored the rate of kinetic energy dissipation in a wind-forced aquatic surface layer. We find that the conventional view, that the dissipation rate corresponds more or less to the scaling appropriate to a turbulent wall layer, is inappropriate when the following conditions are met: (i) the airflow is aerodynami-

cally rough so that the stress is communicated to waves of various lengths and not directly to the surface current; (ii) there is wave breaking [this is always true when (i) occurs]; and (iii) observations are made within a few wave heights of the surface. Under these conditions the dissipation rate is found to scale with the energy flux from the wind to the waves, $\tau_a\bar{c}$, and a wave-dependent length scale, which we have taken to be the significant height of the wind sea H_s. We conjecture that these variables completely describe the dependence of the near-surface dissipation rate on the waves. The total dissipation in the upper layer is then given by $\tau_a\bar{c}$, which is typically an order of magnitude greater than the conventional estimate, $\tau_a u_{*a}/2$, based on shear production.

Our results suggest that the wave-stirred near-surface region is best described by a three-layer structure: The top layer or breaking zone is a region of direct injection of turbulence from wave breaking. Its depth z_b is estimated to be 60% of H_s, and approximately half the total energy dissipation occurs there. Below this lies a layer in which the energy dissipation rate decays with depth as z^{-2}, scales with both wave and wind forcing parameters, and which eventually merges with a deeper layer of slower decay in which wall layer scaling is appropriate. The depth of this transition layer, z_t/H_s, is found to be related to the ratio $\bar{c}/u_{*a}$ (which is equal to the energy flux into the water column due to breaking normalized by $\rho_a u_{*a}^3$). For wave ages typical of this study (i.e., c_p/u_{*a} in the range 4–7) $\bar{c} \sim 0.5c_p$. However, $\bar{c}/u_{*a}$ is found to be a function of wave age and reaches a maximum of 7–8 at an intermediate stage of wave development. Hence, the thickness of the transition layer is dependent on both the significant wave height and the state of the development of the waves and may be as large as $25H_s$ for waves of intermediate development.

The most important contributions of this work are (i) a clear demonstration that the conventional estimates of the dissipation rate of turbulent kinetic energy based on the wall layer analogy ($u_{*w}^3/\kappa z$) are too small by an order of magnitude in moderate and strong winds and (ii) our proposal [embodied in Eqs. (2a,b) and (9)] of a simple wave-dependent scaling of dissipation under these conditions. Furthermore, our revised estimate of the energy flux from the wind, $\tau_a\bar{c}$, emphasizes that this quantity depends on the wave spectrum and its development, underscoring the need for comprehensive and accurate wave measurements in studies of the dynamics of the upper mixed layer. Our results demand new approaches to modeling the many processes of physical, chemical, and biological interest that are linked to the intensity of mixing in the very near surface layers.

Acknowledgments. The participation of A. W., E. T., and Y. A. in the WAVES experiment was originally supported by the U.S. National Science Foundation under Grant OCE-8418711. E. T. received additional support from the U.S. Office of Naval Research under Contract N00014-87-K-007 NR 083-004, and continuing funding from the National Science Foundation under Grant OCE-9301440. M. D., W. D., and K. K. were supported in part by the Panel for Energy Research and Development (Canada), and P. H. by Quest Integrated's internal R&D fund. The authors thank the anonymous referees for their comments and suggestions, and E. T. thanks Dr. J. Trowbridge for helpful discussions. This is NWRI Report 95-010.

REFERENCES

Agrawal, Y. C., and C. J. Belting, 1988: Laser velocimetry for benthic sediment transport. *Deep-Sea Res.*, **35,** 1047–1067.

——, E. A. Terray, M. A. Donelan, P. A. Hwang, A. J. Williams III, W. M. Drennan, K. K. Kahma, and S. A. Kitaigorodskii, 1992: Enhanced dissipation of kinetic energy beneath surface waves. *Nature,* **359,** 219–220.

Anis, A., and J. N. Moum, 1992: The superadiabatic surface layer of the ocean during convection. *J. Phys. Oceanogr.,* **22,** 1221–1227.

——, and ——, 1995: Surface wave–turbulence interactions: Scaling $\epsilon(z)$ near the sea surface. *J. Phys. Oceanogr.,* **25,** 2025–2045.

Arsenyev, S. A., S. V. Dobroklonsky, R. M. Mamedov, and N. K. Shelkovnikov, 1975: Direct measurements of some characteristics of fine-scale turbulence from a stationary platform in the open sea. *Izv. Atmos. Ocean. Phys.,* **11,** 530–533.

Banner, M. L., 1990: Equilibrium spectra of wind waves. *J. Phys. Oceanogr.,* **20,** 966–984.

Birch, K. G., and J. A. Ewing, 1986: Observations of wind waves on a reservoir. Rep. 234, Institute of Oceanographic Sciences, Wormley, Surrey, England, 34 pp.

Churchill, J. H., and G. T. Csanady, 1983: Near-surface measurements of quasi-Lagrangian velocities in open water. *J. Phys. Oceanogr.,* **13,** 1669–1680.

Craig, P. D., and M. L. Banner, 1994: Modeling wave-enhanced turbulence in the ocean surface layer. *J. Phys. Oceanogr.,* **24,** 2546–2559.

Csanady, G. T., 1984: The free surface turbulent shear layer. *J. Phys. Oceanogr.,* **14,** 402–411.

Dillon, T. M., J. G. Richman, C. G. Hansen, and M. D. Pearson, 1981: Near-surface turbulence measurements in a lake. *Nature,* **290,** 390–392.

Donelan, M. A., 1978: On the fraction of wind momentum retained by waves. *Marine Forecasting: Prediction, Modelling and Ocean Hydrodynamics,* J. C. Nihoul, Ed., Elsevier, 141–159.

——, 1990: *The Sea, Ocean Engineering Science,* Vol. 9, Air–Sea Interaction. B. LeMéhauté and D. Hanes, Eds., Wiley and Sons, 239–292.

——, and J. Motycka, 1978: Miniature drag sphere velocity probe. *Rev. Sci. Instrum.,* **49,** 298–304.

——, and W. J. Pierson, 1987: Radar scattering and equilibrium ranges in wind generated waves with applications to scatterometry. *J. Geophys. Res.,* **92,** 4971–5029.

——, J. Hamilton, and W. H. Hui, 1985: Directional spectra of wind-generated waves. *Philos. Trans. Roy. Soc. London, Ser. A,* **315,** 509–562.

Drennan, W. M., K. K. Kahma, and M. A. Donelan, 1992a: The velocity field beneath wind-waves—observations and inferences. *Coastal Eng.,* **18,** 111–136.

——, ——, E. A. Terray, M. A. Donelan, and S. A. Kitaigorodskii, 1992b: Observations of the enhancement of kinetic energy dissipation beneath breaking wind waves. *Breaking Waves,* M. L. Banner and R. H. Grimshaw, Eds., Springer-Verlag, 95–101. *IUTAM Symposium on Breaking Waves,* Sydney, Australia, July, 1991.

——, M. A. Donelan, E. A. Terray, and K. B. Katsaros, 1996: Oceanic turbulence dissipation measurements in SWADE. *J. Phys. Oceanogr.*, **26,** 808–815.

Gargett, A. E., 1989: Ocean turbulence. *Ann. Rev. Fluid Mech.*, **21,** 419–451.

George, R., R. E. Flick, and R. T. Guza, 1994: Observations of turbulence in the surf zone. *J. Geophys. Res.*, **99,** 810–810.

Grant, H. L., R. W. Stewart, and A. Molliet, 1962: Turbulent spectra from a tidal channel. *J. Fluid Mech.*, **12,** 241–268.

Gregg, M. C., 1987: Structures and fluxes in a deep convecting mixed layer. *Dynamics of the Ocean Mixed Layer,* P. Müller and D. Henderson, Eds., Hawaiian Institute of Geophysics, 1–23.

Hasselmann, K., 1974: On the spectral dissipation of ocean waves due to whitecapping. *Bound.-Layer Meteor.*, **6,** 107–127.

——, T. P. Barnett, E. Bouws, H. Carlson, D. E. Cartwright, K. Enke, J. A. Ewing, H. Gienapp, D. E. Hasselmann, P. Kruseman, A. Meerburg, P. Müller, D. J. Olbers, K. Richter, W. Sell, and H. Walden, 1973: Measurements of wind-wave growth and swell decay during the Joint North Sea Wave Project (JONSWAP). *Dtsch. Hydrogr. Z.,* **12,** (Suppl.), 95 pp.

Jeffreys, H., 1924: On the formation of waves by wind. *Proc. Roy. Soc. London,* **A107,** 189–206.

——, 1925: On the formation of waves by wind. II. *Proc. Roy. Soc. London,* **A110,** 341–347.

Jones, I. S. F., 1985: Turbulence below wind waves. *The Ocean Surface—Wave Breaking, Turbulent Mixing and Radio Probing,* Y. Toba and H. Mitsuyasu, Eds., Reidel, 437–442.

——, and B. C. Kenney, 1977: The scaling of velocity fluctuations in the surface mixed layer. *J. Geophys. Res.*, **82,** 1392–1396.

Kahma, K. K., 1981: A study of the growth of the wave spectrum with fetch. *J. Phys. Oceanogr.*, **11,** 1503–1515.

——, and C. J. Calkoen, 1992: Reconciling discrepancies in the observed growth of wind-generated waves. *J. Phys. Oceanogr.*, **22,** 1389–1405.

Kitaigorodskii, S. A., 1984: On the fluid dynamical theory of turbulent gas transfer across an air–sea interface in the presence of breaking wind waves. *J. Phys. Oceanogr.*, **14,** 960–972.

——, M. A. Donelan, J. L. Lumley, and E. A. Terray, 1983: Wave–turbulence interactions in the upper ocean: Part II. *J. Phys. Oceanogr.*, **13,** 1988–1999.

Lumley, J. L., and E. A. Terray, 1983: Kinematics of turbulence convected by a random wave field. *J. Phys. Oceanogr.*, **13,** 2000–2007.

Maat, N., C. Kraan, and W. A. Oost, 1991: The roughness of wind waves. *Bound.-Layer Meteor.*, **54,** 89–103.

Melville, W. K., 1993: The role of breaking in air–sea interaction. *Proc. 18th Int. Congress of Theoretical and Applied Mechanics,* S. R. Bodner, Ed., Elsevier, 99–117.

——, 1994: Energy dissipation by breaking waves. *J. Phys. Oceanogr.*, **24,** 2041–2049.

Miles, J. W., 1957: On the generation of surface waves by shear flows. *J. Fluid Mech.*, **3,** 185–204.

Mitsuyasu, H., 1985: A note on the momentum transfer from wind to waves. *J. Geophys. Res.*, **90,** 3343–3345.

Oakey, N. S., and J. A. Elliott, 1982: Dissipation within surface mixed layer. *J. Phys. Oceanogr.*, **12,** 171–185.

Osborn, T., D. M. Farmer, S. Vagle, S. Thorpe, and M. Cure, 1992: Measurements of bubble plumes and turbulence from a submarine. *Atmos.–Ocean,* **30,** 419–440.

Phillips, O. M., 1985: Spectral and statistical properties of the equilibrium range in wind-generated gravity waves. *J. Fluid Mech.*, **156,** 505–531.

Plant, W. J., 1982: A relationship between wind stress and wave slope. *J. Geophys. Res.*, **87,** 1961–1967.

Rapp, R. J., and W. K. Melville, 1990: Laboratory measurements of deep-water breaking waves. *Philos. Trans. R. Soc. London,* **A331,** 735–800.

Soloviev, A. V., N. V. Vershinsky, and V. A. Bezverchnii, 1988: Small-scale turbulence measurements in the thin surface layer of the ocean. *Deep-Sea Res.*, **35,** 1859–1874.

Stewart, R. W., and H. L. Grant, 1962: Determination of the rate of dissipation of turbulent energy near the sea surface in the presence of waves. *J. Geophys. Res.*, **67,** 3177–3180.

Terray, E. A., and L. F. Bliven, 1985: The vertical structure of turbulence beneath gently breaking wind waves. *The Ocean Surface: Wave Breaking, Turbulent Mixing and Radio Probing,* Y. Toba and H. Mitsuyasu, Eds., D. Reidel, 395–400.

Thorpe, S. A., 1993: Energy loss by breaking waves. *J. Phys. Oceanogr.*, **23,** 2498–2502.

Tsanis, I. K., and M. A. Donelan, 1989: Wave directional spectra in mixed seas. *Proc. Second Int. Workshop on Wave Hindcasting and Forecasting,* Vancouver, Environment Canada, AES-Downsview, 387–396.

Williams, A. J., III, 1985: BASS, an acoustic current meter for benthic flow-field measurements. *Mar. Geol.*, **66,** 345–355.

Wu, J., 1975: Wind-induced drift currents. *J. Fluid Mech.*, **68,** 49–70.